International Journal of Pharmacy and Biological Sciences-IJPBS™ (2021) 11 (4): 76-87
Online ISSN: 2230-7605, Print ISSN: 2321-3272
Research Article | Biological Sciences | OA Journal | MCI Approved | Index Copernicus

Thymoquinone Loaded Solid Lipid Nanoparticles Exhibit Cytoprotective Effect Against 3-Nitropropionic Acid Exposed Changes In SHSY-5Y Neuroblastoma Cells

Surekha Ramachandran[1] and Sumathi Thangarajan[2]*

[1]Department of Biochemistry, SRM Dental College, Ramapuram, Chennai-600 089, Tamil Nadu, India.

[2]Department of Medical Biochemistry, Dr. ALM Post Graduate Institute of Basic Medical Sciences, University of Madras, Taramani Campus, Chennai-600 113, Tamil Nadu, India.

Received: 12 Jul 2021/ Accepted: 06 Aug 2021 / Published online: 1 Oct 2021
*Corresponding Author Email: drsumathi.bioscience@gmail.com

Abstract

The present study investigated the cytotoxic events upon 3-Nitropropionic acid (3-NP) exposure and the protective effect of thymoquinone nano formulation (TQ-SLNs) in SH-SY5Y neuroblastoma cells. The SH-SY5Y neuroblastoma cells were incubated separately for 1 hr. with TQ-SLNs (0.4 µM) and TQ (5 µM) in 96-well plates, and then the cells were exposed to 3-NP (0.5 mM) for 24 hrs. Exposure of 3-NP (0.5 mM) reduced the cell viability and antioxidant GSH level with a concurrent increased release of LDH in the cytosol. 3-NP exposure also causes loss in Mitochondrial Membrane Potential (MMP) with increased content of cytosolic cytochrome *c*. The apoptotic incidence upon 3-NP exposure was also evident as an increased nuclear condensation in Hoechst 33342 and Acridine orange/Ethidium bromide staining. On the other hand, TQ-SLNs treatment effectively increased the percentage of cell viability, GSH level, preserved the MMP, controlled the LDH and cytochrome *c* release, and reduced the nuclear condensation. TQ-SLNs also found to regulate the cell cycle process, which was found arrested at G0/G1 phase during 3-NP exposure. From the result, we suggest that TQ-SLNs could effectively exhibit beneficial action against cell injury during 3-NP challenged condition.

Keywords

Thymoquinone, Solid lipid nanoparticles, 3-Nitropropionic acid, Mitochondrial dysfunction, SH-SY5Y neuroblastoma cells

*****

1. INTRODUCTION

3-nitropropionic acid (3-NP) is a mycotoxin, obtained from fungi and plants and is widely used to mimic Huntington's disease (HD) pathogenesis in an *in vivo* model [1]. HD is an autosomal dominant neurodegenerative disease characterized by the motor, cognitive, and psychiatric disturbances [2,3]. Among various neurotoxins, 3-NP is considered to be the most effective model to develop HD-like symptoms because it could directly cross Blood Brain Barrier (BBB) and creates bilateral striatal lesion [4]. The mechanism of 3-NP involves an irreversible inhibition of succinate dehydrogenase (SDH) enzyme in both mitochondrial tricarboxylic acid cycle (TCA) and electron transport chain (ETC) leading to ATP depletion and energy failure [5]. It also triggers calcium dyshomeostasis, excitotoxic events,

oxidative stress, mitochondrial dysfunction, inflammation, and cell death [4,6].

Thymoquinone (TQ) (2-isopropyl-5-methyl-1, 2-benzoquinone), a major bioactive compound of *Nigella sativa* seeds, is reported to have various pharmacological applications such as antioxidant [7], anti-inflammatory [8], immunomodulatory [9] and hepatoprotective properties [10]. TQ also showed a neuroprotective efficacy against ethanol-induced cytotoxicity in primary rat cortical neurons [11]. Further, Mousavi et al. [12] reported that TQ protects the PC12 cells against cytotoxic glucose deprivation via quenching reactive oxygen species (ROS) generation. TQ also protected the cultured rat primary neurons against amyloid beta ($A\beta_{1-42}$) peptide and dopaminergic neurons against MPP^+ and rotenone exposed cytotoxicity [13,14]. Further, TQ displayed an anti-convulsant [15], anti-anxiety [16] and anti-depression-like effect [17] in various experimental animal models. Regardless of numerous therapeutic applications, this active compound suffers from the disadvantage of poor bioavailability and water solubility, which was potentiated using a suitable carrier, solid lipid nanoparticles (SLNs). SLNs constitute physiological and biocompatible lipids with controlled drug release potency and remains a universally specified drug carrier to the central nervous system (CNS) [18,19]. Therefore, thymoquinone-loaded solid lipid nanoparticles (TQ-SLNs) were formulated and their physico-chemical characteristics were studied [20,21]. An *in vivo* pharmacodynamic strategy of TQ-SLNs were employed against 3-NP neurotoxicity and was determined to be more effective than thymoquinone suspension [22]. To this context, the crucial insights about the post-mitochondrial inhibitory events and cytotoxic mechanism of 3-NP and the preventive role of TQ-SLNs formulation were extensively studied using a potential research tool, the SH-SY5Y neuroblastoma cells.

2. MATERIALS AND METHODS

2.1. Chemicals and Reagents

3-Nitropropionic acid, Thymoquinone, dimethyl sulfoxide (DMSO) and 3-(4,5-dimethylthiazol-2-yl)-2,5-diphenyltetrazolium bromide (MTT) were purchased from Sigma-Aldrich (St. Louis, USA). Stearic acid, Soy Lecithin and Sodium taurocholate were purchased from Himedia Laboratories Pvt. Ltd. (Mumbai, India). SH-SY5Y cell lines were procured from National Centre for Cell Science (NCCS), Pune, India. Modified Dulbecco's Eagle's medium (DMEM) supplement with ham's F12 was obtained from Himedia Laboratories Pvt. Ltd. (Mumbai, India). Heat-inactivated fetal bovine serum (FBS), streptomycin, penicillin, and trypsin-EDTA were obtained from Invitrogen Corporation (California, USA). The cell culture (96-well and 6-well) plates and culture flasks (25 cm^2 × 75 cm^2) were purchased from Himedia Pvt. Ltd. (Mumbai, India).

2.2. Preparation of Thymoquinone-loaded Solid Lipid Nanoparticles (TQ-SLNs)

Stearic acid at a mole fraction of 0.710 was allowed to melt at ~75°C. Simultaneously, distilled water was heated at ~75°C in a separate beaker, to which lecithin, taurocholate and thymoquinone at a mole fraction of 0.210, 0.069 and 0.011 respectively, were added and stirred mechanically. The water–surfactant solution was then added to the melted lipid and maintained at ~75°C. The mixture was then homogenized at 24,000×g for 150 s to form the emulsion. The obtained hot microemulsion was added into an ice-cold water (~2°C), at a ratio of 1:20 (warm microemulsion/cold water) under constant stirring resulting in the formation of solidified lipid nanoparticles, which was centrifuged at 20,000×g for 15 min and the nanoparticle pellet was resuspended in distilled water. The preparation was stored at 4°C for further analysis [23].

2.3. Cell Culture Treatment

The SH-SY5Y neuroblastoma cells were cultured in the flask containing DMEM enriched with 10% (v/v) heat inactivated FBS, 100 µg/ml penicillin, and 100 µg/ml streptomycin incubated at 37°C in 5% CO_2 incubator [24]. After 80 to 90% confluence in the flask, the cells were trypsinized and seeded on to the fresh plates. Preliminary studies were carried out to determine 50% inhibitory concentration (IC_{50}) of 3-NP at different concentrations (0.1, 0.2, 0.3, 0.4, 0.5, 1.0, 5.0, 10.0, and 20.0 mM) for 24 hrs, similarly, TQ-SLNs and TQ at 0.1, 0.2, 0.3, 0.4, 0.5, 1.0, 5.0, 10.0, and 20.0 µM concentrations were determined by incubating the cells for a period of 24 hrs.

2.4. Determination of Cell Viability

The MTT reduction assay was performed to assess the viability of cells [25]. Differentiated SH-SY5Y cells (2 × 10^4 cells/well in 96-well plates) were incubated with TQ-SLNs (0.4 µM) and TQ (5.0 µM) for 1 hr and then exposed to 3-NP (0.5 mM) for 24 hrs. After 24 hrs of incubation, 20 µl of MTT stock standard solution with a concentration of 5 mg/ml was added and incubated for 4 hrs at 37°C. The reaction was arrested using 150 µl of DMSO reagent and the color absorbance was read at 540 nm in a microtiter plate reader. The percentage of viable cells can be calculated using the formula,

$$\% \text{ Viability} = \frac{\text{Mean Absorbance of Sample}}{\text{Mean Absorbance of Negative Control}} \times 100$$

2.5. Measurement of Lactate Dehydrogenase (LDH)

LDH is a cytosolic enzyme which was assessed in the culture medium to determine the loss of plasma membrane integrity and cell death. The SH-SY5Y cells (2×10^4 cells/well in 96-well plates) were treated with 3-NP (0.5 mM) for 24 hrs with or without TQ-SLNs (0.4 µM) and TQ (5.0 µM) pretreatment. The cells were then harvested using 0.1% trypsin-EDTA and centrifuged at 3000 × g to cause cell lysis. After centrifugation, the clear supernatant was collected, and measured for the activity of LDH. The release of LDH from the cells was analyzed by LDH cytotoxicity assay kit (Cayman Chemical, USA) according to the manufacturer's protocol.

2.6. Analysis of Cellular Morphology by Phase Contrast Microscopy

The SH-SY5Y cells were exposed to 3-NP (0.5 mM) with or without TQ-SLNs (0.4 µM) and TQ (5.0 µM) for 24 hrs and observed under a phase contrast microscopy at 20 µm scale bar to determine the morphological abnormalities. The medium was changed before the microscopic examination to avoid the interference of dead cells.

2.7. Measurement of Intracellular Anti-oxidative Glutathione

The reduced glutathione level (GSH) in cell lysate was determined using o-phthalaldehyde (OPT) [26]. The SH-SY5Y cells at a density of (2×10^4 cells/well in 96-well plates) were exposed to 3-NP (0.5 mM) with or without TQ-SLNs (0.4 µM) and TQ (5.0 µM) pre-treatment for 24 hrs followed by PBS wash thrice. The cells were lysed by vigorous shaking with 500 µl buffer containing 0.2% Triton-X 100 and 5 mmol/L EDTA (pH 8.3). After cell lysis, 0.3 ml of supernatant was removed and mixed with 0.1 ml of 20% trichloroacetic acid (TCA), and centrifuged at 200 × g for 10 min. The supernatant was collected and incubated with 50 mg/L OPT (dissolved in DMSO and diluted to the final concentration with PBS) for 15 min at 37°C and the fluorescence was measured spectrofluorimetric at an excitation wavelength of 350 nm and emission wavelength of 420 nm.

2.8. Determination of Mitochondria Membrane Potential (MMP) using Rhodamine 123 Stain

The mitochondrial membrane potential was examined microscopically by the fluorescent dye Rhodamine 123 (Rh-123) [27]. SH-SY5Y cells were seeded in 6-well plates at a density of 1×10^5 cells/mL and exposed to 3-NP (0.5 mM) with or without TQ-SLNs (0.4 µM) and TQ (5.0 µM) pre-treatment for 24 hrs. After incubation, Rh-123 (10 µg/ml) was added to the medium and incubated for 30 min at 37°C. After incubation, the cells were washed and re-suspended in PBS, and observed under fluorescent microscopy (Nikon, Eclipse TS100, Japan) with the excitation wavelength at 488 nm and the emission wavelength at 523 nm.

2.9. Quantification of Cytosolic Cytochrome c

The release of cytochrome *c* (cyt *c*) from the mitochondria was analyzed in the cells exposed to 3-NP (0.5 mM) with or without TQ-SLNs (0.4 µM) and TQ (5.0 µM) pretreatment for 24 hrs. After 24 hrs treatment, the cells were homogenized, and the cell lysate was centrifuged at 7,000 × g for 5 min at 4°C. The pellet containing nucleus and unbroken cells was discarded and the supernatant was then centrifuged at 12,000 × g for 15 min at 4°C. The resultant supernatant containing crude cytosolic fraction was again centrifuged at 14,000 × g for 20 min at 4°C. The uppermost part of the supernatant was separated (cytosolic fraction) and analyzed for protein content by the method of Lowry et al. [28] verifying equal amount of protein content for cyt *c* estimation. The concentration of cytochrome *c* in the supernatant was measured using a Quantikine cytochrome *c* ELISA kit (Minneapolis, USA) according to the manufacturer's instruction. Samples were run in triplicate and the cyt *c* release was expressed as a fold of the level of cytochrome c present in the cytosol of control cells [29].

2.10. Detection of Nuclear Morphological Changes and Cell Death by Hoechst 33342 Stain

The changes in the nuclear morphology and apoptosis of SH-SY5Y cells were visualized using Hoechst 33342 stain [30]. The SH-SY5Y cells were seeded on to the 6-well plate at a density of 1×10^5 cells/mL and treated with TQ-SLNs (0.4 µM) and TQ (5.0 µM) for 1.5 hrs prior to the exposure of 3-NP (0.5 mM) and incubated for a period of 48 hrs. The cells were then fixed with 4% paraformaldehyde, washed and stained using 5 µg/mL Hoechst 33342 stain for a period of 30 min at 37°C. The excess stain was removed by washing the cells twice with PBS and viewed to examine nuclear morphology under a fluorescence microscope (Nikon, Eclipse TS100, Japan) with the excitation wavelength at 355 nm and the emission wavelength at 465 nm.

2.11. Determination of Apoptotic Cell Death by Acridine Orange/Ethidium Bromide Dual Stain

The acridine orange (AO) and ethidium bromide (EtBr) stains were used to visualize the condensed chromatin of apoptotic cells [31]. The SH-SY5Y cells

were seeded in a 6-well plate (1×10^5 cells/mL) and treated with TQ-SLNs (0.4 µM) and TQ (5.0 µM) for 1.5 hrs prior to the exposure of 3-NP (0.5 mM) for a period of 48 hrs. After 48 hrs incubation, the cells were fixed using the mixture containing methanol and acetic acid (glacial) in the ratio of 3:1 for 30 min at 37°C and washed with PBS. The cells were then stained with AO/EtBr at a ratio of 1:1. The staining mixture was prepared using 100 µl of 1 mg/ml AO (Sigma-Aldrich Company Co., USA) and 100 µl of 1 mg/ml EtBr (Sigma-Aldrich Company Co., USA). The AO/EtBr-stained cells were then washed twice with PBS to remove excessive stain and visualized under fluorescence microscope (Nikon, Eclipse TS100, Japan) with the excitation wavelength at 460 nm and the emission wavelength at 650 nm.

2.12. Analysis of Cell Cycle Arrest by Flow Cytometry

SH-SY5Y cells were seeded in 96-well plates at density of 1×10^5 cells/mL and exposed to 3-NP (0.5 mM) with or without TQ-SLNs (0.4 µM) and TQ (5.0 µM) pretreatment for 24 hrs and analyzed by flow cytometry with propidium iodide (PI) staining Kit (Cayman Chemicals, USA). After 24 hrs, the cells were washed with an ice-cold PBS and centrifuged at 1500 × g for 5 min and suspended in 500 µl of binding buffer. Then the cells were treated with FITC-labelled PI (5 µl) and incubated at 37°C for 15 min according to the manufacturer's instruction. The cells arrested in different stages were measured with FACSCalibur flowcytometer (Becton Dickinson, USA). The cells were counted in single cell gate of 10,000 events and the graph was plotted against area and counts to analyze percentage (%) gating [32].

2.13. Statistical Analysis

Data were presented as mean ± standard error of mean (SEM) of at least three to six independent experiments. Data were analyzed using one way analysis of variance (ANOVA) followed by Tukey's *Post-hoc* test (SPSS 20 version). Values with $P<0.05$ were considered to be statistically significant.

3. RESULTS

3.1. Effect of TQ-SLNs and TQ on 3-NP induced Cytotoxicity in SH-SY5Y cells

The 3-NP induced cytotoxicity was evaluated by MTT reduction assay. Figure 1A, 1B, 1C depicted the concentration-response percentage of cell viability upon exposure to 3-NP, TQ-SLNs and TQ, where the IC_{50} concentration of 3-NP was noted to be 0.5 mM and used for further studies. Similarly, the IC_{50} concentration upon treatment with TQ-SLNs and TQ was observed to be 0.4 µM and 5.0 µM respectively. Further, the cytoprotective effect of TQ-SLNs and TQ against 3-NP were studied, where 3-NP significantly ($P<0.01$) decreased the presence of survival cells. TQ-SLNs (0.4 µM) treatment improved the cell viability significantly ($P<0.01$) compared to TQ (5.0 µM) treatment (Figure 1D).

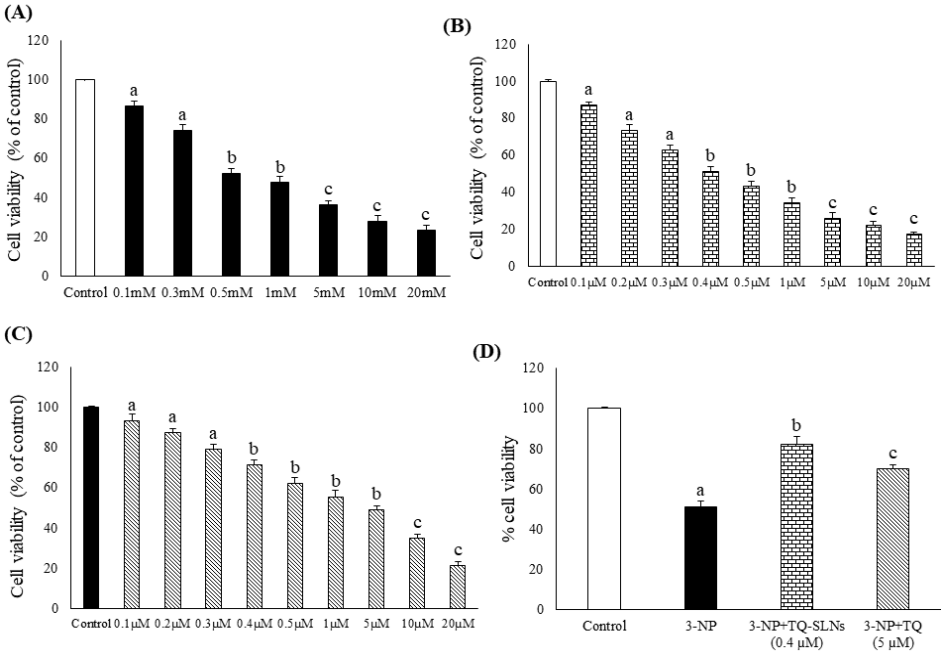

Figure 1. TQ-SLNs pre-treatment ameliorates cytotoxicity in 3-NP exposed SH-SY5Y cells. Representative bar images demonstrating the cytotoxicity of varying concentration of 3-NP exposed (A), TQ-SLNs treated (B), TQ treated (C) SH-SY5Y cells. Figure D depicts the effect of TQ-SLNs and TQ on 3-NP exposed cytotoxicity in SH-SY5Y cells. Data represent mean ± SEM from three independent experiments. Units were expressed as % cell viability. a$P < 0.01$ compared to control cells; b$P < 0.01$, c$P < 0.05$ compared to 3-NP exposed cells (One way ANOVA followed by Tukey's Post-hoc test).

3.2. Effect of TQ-SLNs and TQ on 3-NP induced LDH leakage in SH-SY5Y cells

Lactate dehydrogenase (LDH) release is an index of cell membrane integrity loss. The exposure of SH-SY5Y cells to 3-NP (0.5 mM) for 24 hrs resulted in a significant (P<0.01) disruption in the cell plasma membrane, which was depicted as an increased release of LDH up to 48.35 ± 2.64% when compared to control cells, where control cells showed 13.62 ± 1.27% of LDH content in the medium. The culture medium of TQ-SLNs and TQ showed a reduced LDH level of 26.62 ± 1.97% in TQ-SLNs (0.4 µM) and 34.25 ± 2.01% in TQ (5.0 µM) treatment when compared to 3-NP exposed cells.

3.3. Effect of TQ-SLNs and TQ on 3-NP induced Morphological abnormalities in SH-SY5Y cells

Morphological studies are important to understand the cytotoxic impact of 3-NP with respect to apoptosis. 3-NP exposed cells exhibited reduced cell numbers and most cells lost neuritis, observed as round shape and increased number of cells were lysed and/or replaced by debris, where control cells showed a normal SH-SY5Y cellular morphology (Figure 2A, 2B). TQ-SLNs (0.4 µM) pre-treatment mitigated such morphological abnormalities derived during 3-NP exposure and showed an increased presence of normal cells with a reduced content of debris (Figure 2C). Cells pre-treated with TQ (5.0 µM) showed a viable cell with slight structural abnormality upon 3-NP challenged condition (Figure 2D).

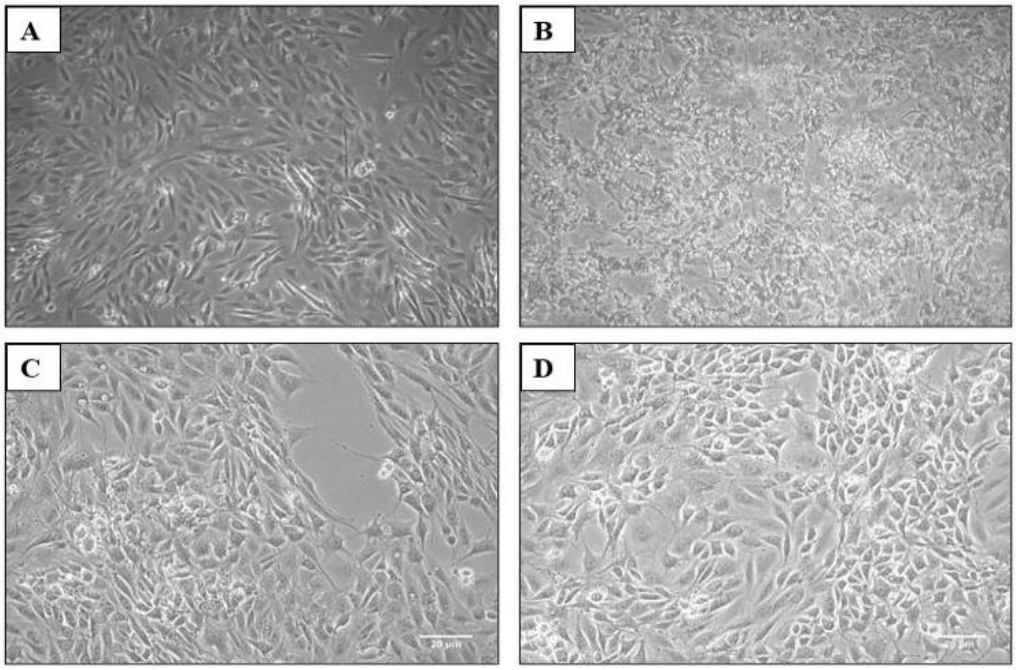

Figure 2. TQ-SLNs pre-treatment protects the cellular morphology of 3-NP exposed SH-SY5Y cells. The cells incubated with 3-NP and/or TQ-SLNs and TQ were visualized and photographed under phase contrast microscopy. (A) Control cells exhibiting normal morphology. (B) 3-NP exposed cells showing retraction of cytoplasm and shrinkage and an increased number of lysed cells and/or replaced by debris. (C) TQ-SLNs (0.4 µM) pre-treatment showing the normal confluence of cells with slight modification in their morphology. (D) TQ (5.0 µM) pre-treated cells showing partially reverted morphological changes with the presence of cell clumping and debris. The scale bar is 20 µm.

3.4. Effect of TQ-SLNs and TQ on 3-NP induced Intracellular GSH level in SH-SY5Y cells

The control cells showed an intracellular GSH content of 87.86 ± 4.12% MFI (mean fluorescence intensity), where the SH-SY5Y cells incubated with 3-NP (0.5 mM) for 24 hrs showed a relative drop in the intracellular GSH to 52.32 ± 3.25% MFI of control values. Pre-treatment with TQ-SLNs (0.4 µM) significantly (P<0.01) increased the basal level of GSH as 75.21 ± 4.32% MFI, where TQ (5.0 µM) pre-treated cells showed a basal level of GSH as 68.35 ± 3.85% MFI when compared to 3-NP exposed cells.

3.5. Effect of TQ-SLNs and TQ on 3-NP induced loss of mitochondrial membrane potential (MMP) in SH-SY5Y cells

The MMP analysis was done using the fluorescent dye Rhodamine 123 (Rh-123), which preferentially partitions active mitochondria containing cells from injured cells. In the present study, the MMP of SH-SY5Y cells was found to be reduced rapidly when

exposed to 3-NP (0.5 mM) (Figure 3B), which was verified as a weak fluorescence intensity when compared to control cells (Figure 3A). Pre-treatment with TQ-SLNs (0.4 µM) protected the cellular mitochondria by showing increased number of Rh-123 stained positive cells (Figure 3C). TQ (5.0 µM) pre-treated cells showed a presence of damaged cells and few normal cells with intact mitochondria (Figure 3D).

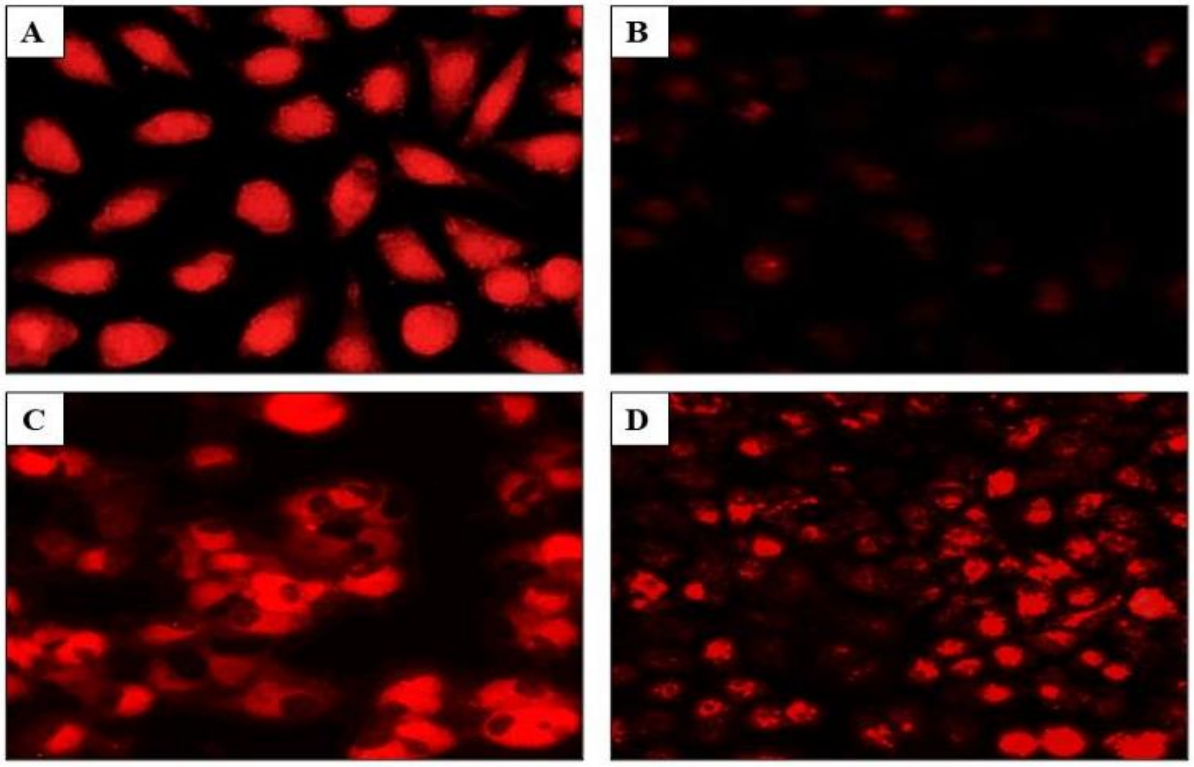

Figure 3. TQ-SLNs pre-treatment protects the Mitochondrial Membrane Potential (MMP) of 3-NP exposed SH-SY5Y cells. Detection of MMP using Rhodamine 123 fluorescent dye. (A) Control cells showing normal Rh-123 fluorescence. (B) 3-NP exposed cells showing decreased fluorescent intensity representing MMP loss. (C) TQ-SLNs (0.4 µM) pre-treated cells showing increased fluorescent intensity by intensive accumulation of Rh-123 stain. (D) TQ (5.0 µM) pre-treated cells showing markedly reduced fluorescent intensity than TQ-SLNs exposed cells when compared to 3-NP exposed cells. The scale bar 20 µm.

3.6. Effect of TQ-SLNs and TQ on 3-NP induced Cytochrome c content in SH-SY5Y cells

Cytochrome *c* is a water-soluble protein loosely attached in the mitochondrial intermembrane space and functions as an electron carrier in electron transport chain. Here, the SH-SY5Y cells treated with 3-NP (0.5 mM) for 24 hrs showed a significantly (P<0.01) increased content of 9.74 ± 0.36 ng/ml cytosolic cyt *c* when compared to control cells, where control cells showed a cytosolic cyt *c* content of 3.05 ± 0.42 ng/ml. Pre-treatment with TQ-SLNs (0.4 µM) resulted in a significant (P<0.01) decrease in the level of cyt *c* of 5.23 ± 0.22 ng/ml, where TQ (5.0 µM) pre-treated cells showed a cytosolic cyt *c* content of 7.24 ± 0.34 ng/mg when compared to 3-NP exposed cells.

3.7. Effect of TQ-SLNs and TQ on 3-NP induced Nuclear Condensation in SH-SY5Y cells by Hoechst 33342 stain

The Hoechst 33342 staining of 3-NP (0.5 mM) incubated cells revealed an appearance of a typical apoptotic characteristics such as chromatin condensation and blebbing (Figure 4B), where control cells showed a normal nuclear morphology (Figure 4A). TQ-SLNs (0.4 µM) pre-treatment cells showed a reduction in the sequences of apoptosis upon 3-NP exposure as compared to TQ (5.0 µM) treatment (Figure 4C, 4D).

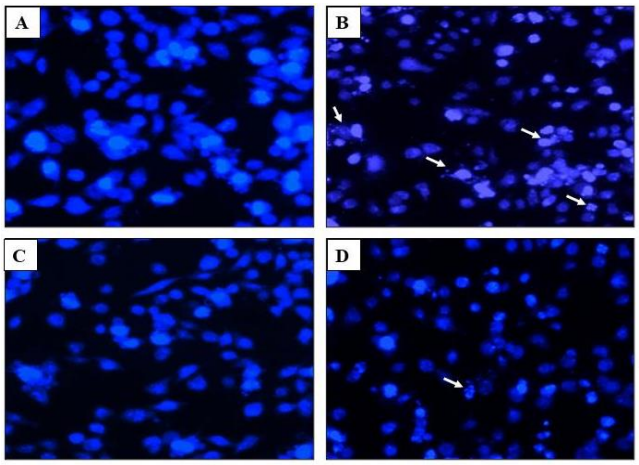

Figure 4. TQ-SLNs pre-incubation suppresses Hoechst 33342 stained nuclear condensation in 3-NP exposed SH-SY5Y cells. Damages in the nucleus were observed using Hoechst 33342 staining. (A) Control cells showing normal nuclear morphology. (B) 3-NP exposed cells showing apoptotic characteristics, such as highly condensed and fragmented nuclei and cell blebbing (denoted by an arrow). (C) TQ-SLNs (0.4 µM) pre-treated cells showing declined number of apoptotic cells compared to the cells exposed with 3-NP. (D) TQ (5.0 µM) pre-treated cells showing a presence of few apoptotic nuclei cells when compared to 3-NP treated cells (denoted by an arrow). The scale bar is 20 µm.

3.8. Effect of TQ-SLNs and TQ on 3-NP induced Apoptotic Cell Death in SH-SY5Y cells by Acridine Orange (AO)/Ethidium Bromide (EtBr) dual stain

In the present study, the fluorescent microscopic visualization of AO-stained control SH-SY5Y cells showed a green, round, intact nucleus. During EtBr staining, untreated control cells revealed an evenly distributed orange fluorescence, which indicate that untreated cells do not undergo apoptosis (Figure 5A 1,2&3). 3-NP (0.5 mM) exposed cells showed a reduced presence of AO-stained normal cells, in addition to the presence of reddish-orange colored (EtBr-positive) cells, indicating the cells that underwent apoptosis (Figure 5B 1,2&3). TQ-SLNs (0.4 µM) treatment (Figure 5C 1,2&3) markedly reduced the occurrence of early and late apoptotic changes by evidencing increased presence of AO probed cells and reduced EtBr probed cells upon 3-NP challenged condition as compared to TQ (5.0 µM) treatment (Figure 5D 1,2&3).

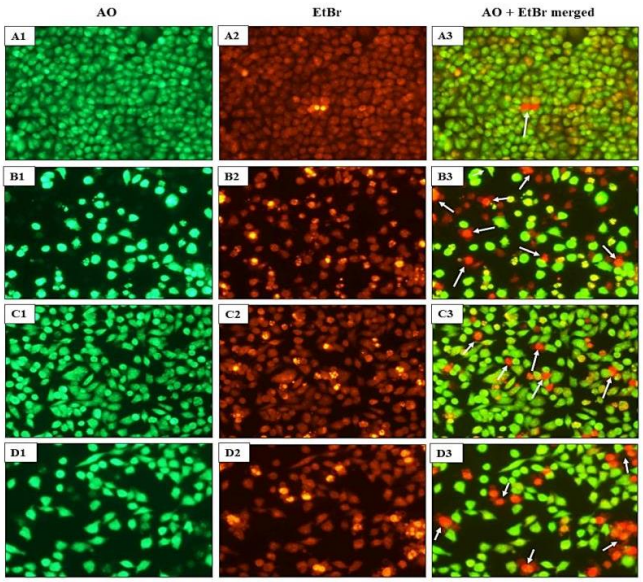

Figure 5. TQ-SLNs pre-treatment reduces Acridine orange (AO)/Ethidium bromide (EtBr) stained apoptotic damages in 3-NP exposed SH-SY5Y cells. Photomicrographs showing the anti-apoptotic effect of TQ-SLNs and TQ against 3-NP exposed apoptosis in SH-SY5Y cells. Figure 5A (1,2,3) Control cells showing the maximum number of viable cells with AO staining indicating intact nucleus and EtBr staining showing evenly distributed orange stain. Figure 5B (1,2,3) 3-NP exposed cells showing an increased number of EtBr-stained cells,

indicating apoptotic cell death, whereas AO-stained cells exhibiting reduced presence of normal cells. Figure 5C (1,2,3) TQ-SLNs (0.4 µM) pre-treated cells showing negligible nuclear condensation and less AO/EtBr staining. Figure 5D (1,2,3) TQ (5.0 µM) pre-treated cells showing apoptotic cells with the presence of normal viable cells. Arrow marks pointing bright, orange-colored cells representing late apoptotic cells. The scale bar is 20 µm.

3.9. Effect of TQ-SLNs and TQ on 3-NP induced Cell Cycle Arrest in SH-SY5Y cells

The result of 3-NP (0.5 mM) incubation exhibited a cell cycle arrest at G0/G1 phase in SH-SY5Y cells, which was depicted as an increased accumulation of the cells at G0/G1 phase and the depleted cell population at S and G1/M phase when compared to control cells (Figure 6A, 6B). However, pre-treatment with TQ-SLNs (0.4 µM) found to regulate the cell-cycle arrest (Figure 6C), which was depicted as an elevated cell counts observed at S and G1/M phase upon 3-NP exposed condition as compared to TQ (5.0 µM) treatment (Figure 6D). The percentage of cell distribution in each phase of cell cycle with significant differences was depicted in Table 1.

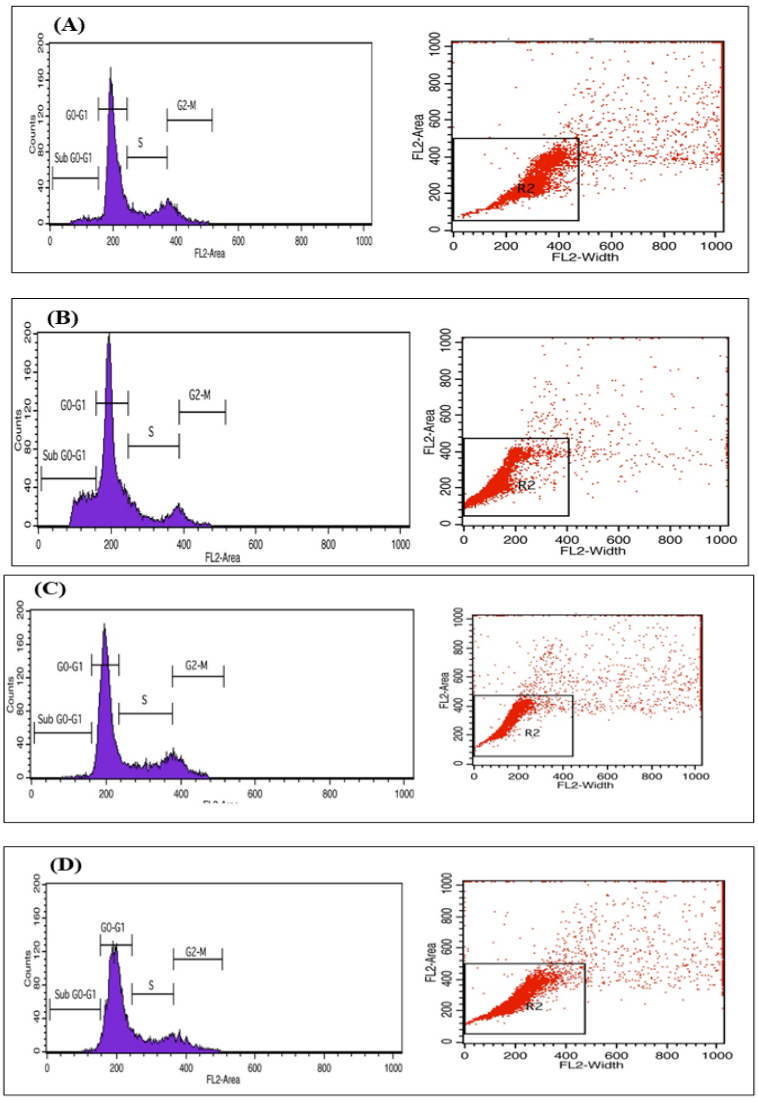

Figure 6. TQ-SLNs pre-treatment regulates 3-NP exposed cell cycle arrest in SH-SY5Y cells. Accumulation of cells in varying cell cycle phases were analyzed by flow cytometry using propidium iodide probe. Representative graphs showing the cell counts in different phases of cell cycle. (A) Control cells showing normal cell cycle distribution. (B) 3-NP exposed cells showing increased percentage of cells that are arrested in the G0/G1 phase of the cell cycle. (C) TQ-SLNs (0.4 µM) pre-treated cells regulated the cell cycle population that has been arrested at G0/G1 phase upon 3-NP exposure. (D) TQ (5.0 µM) pre-treated cells also prevented the cell cycle arrest at G0/G1 phase.

Table 1. Percentage of Cell Distribution in Different Phases of Cell Cycle

Groups	Control	3-NP	3-NP + TQ-SLNs (0.4 µM)	3-NP + TQ (5 µM)
Marker	Gated %	Gated %	Gated %	Gated %
All	100	100.00	100.00	100.00
Sub G0-G1	1.77	20.42[a]	2.02[b]	1.28[b]
G0-G1	64.78	85.97[a]	70.71[b]	79.66[c]
S	15.51	5.63[a]	12.89	11.27
G2-M	5.38	1.89[a]	3.03	2.90

Data represents mean ± SEM (n=3). aP < 0.01 compared to control cells, bP < 0.01, cP < 0.05 compared to 3-NP exposed cells (One way ANOVA followed by Tukey's Post-hoc test).

4. DISCUSSION

Mitochondria plays a significant role in the process of apoptosis and also in neurodegeneration [33]. Disruption of mitochondrial activity is associated with the abnormal generation of ROS leading to oxidative stress [34]. Mitochondrial dysfunction caused by ROS-induced oxidative damage has been shown to involve in the development of apoptotic cell death in HD as well as in 3-NP toxicity [35,36]. The present study was framed to explore the effect of TQ-SLNs and TQ on mitochondrial inhibitory events associated cell death in 3-NP challenged condition using SH-SY5Y cells. The cytoprotective activity of TQ-SLNs and TQ were determined by MTT assay. Exposure of 3-NP to the cells in our study causes inhibition of growth and metabolic activity in a dose-dependent manner, which was antagonized upon treatment with TQ-SLNs and represented as increased number of viable cells than TQ exposed group. The cytoprotective effect of TQ-SLNs was obtained by regulating the metabolic function and quenching the free radical generation that in-turn helps in maintaining the cellular integrity and viability. Further, the phase contrast microscopic visualization of TQ-SLNs pre-treated cells confirmed the presence of greater number of cells with intact morphology, demonstrating the cytoprotective potency of TQ-SLNs than TQ against 3-NP toxicity.

The LDH assay was considered to be a highly sensitive cytotoxicity test used to quantify changes in the total cell number or the cell membrane integrity [37]. LDH is a cytosolic enzyme that gets rapidly released into the culture medium upon cell lysis or damage [38]. In our study, upon 3-NP exposure there was a rapid increase in the release of LDH in the culture medium indicating cytotoxicity. However, TQ-SLNs prevented the release of LDH via maintaining the integrity of the cellular plasma membrane through its antioxidant potency.

Further, the antioxidant potential of TQ-SLNs was determined by estimating the level of GSH content. GSH is the most abundant cellular thiol antioxidant which plays a central role in maintaining cellular redox status and increase in GSH levels would be expected to reduce ROS levels and antagonize apoptotic signal [39]. To this instance, the present data signifies the inability of the cells to stimulate GSH, which may likely relate the stringent regulation of cellular glutathione redox status in SH-SY5Y cells upon 3-NP incubation. Further, TQ-SLNs pre-treatment than TQ could significantly elicit a glutathione antioxidant response to scavenge free radicals to afford cytoprotection against oxidative stress during 3-NP-challenged condition.

Collapse in Mitochondrial Membrane Potential (MMP) provide an early indication of cellular apoptosis, where 3-NP exposure causes depolarization of mitochondrial membrane by stimulating complexes inhibition and free radical generation [40]. In order to determine the mitochondrial membrane potential loss and concentration gradients, Rh-123 was used as a potential marker [41]. Our study depicted a lowered number of Rh-123 positive cells in 3-NP exposed condition, verifying MMP depolarization. Further, an enhanced depolarization of mitochondrial membrane triggers an opening of transition pore, leading to cyt *c* release from the mitochondria into cytosol. Release of cyt *c* in cytosol activates the downstream caspase cascade, leading to apoptosis [42]. Nevertheless, the preservation of mitochondrial function was attained effectively upon TQ-SLNs pre-treatment depicted as an increased rhodamine fluorescence, which was achieved by inhibiting the ETC dyshomeostasis-mediated ROS generation in the mitochondria. Further, the preservation of mitochondrial membrane inhibited the release of cyt *c* into cytosol, hence protecting the cells from the event of apoptosis.

The mitochondrial dysfunction mediated apoptosis was further evidenced using Hoechst 33342 stain. Hoechst 33342 assay, a classic method to distinguish apoptotic cells, normal cells, and necrotic cells [43]. A small amount of Hoechst 33342 could penetrate the normal cell membranes and emit dark blue fluorescence upon combination with DNA. However,

lighter blue fluorescence was emitted in the apoptotic cells, because of membrane permeability enhancement, DNA breakage and inactivation of P-glycoprotein [44]. On the other hand, the AO/EtBr staining was performed, where AO is a cell-permeant nucleic acid binding dye which emits green fluorescence when interacting with double standard DNA, and red fluorescence when interacting with single standard DNA or RNA. EtBr believed to stain the cells that lack nuclear membrane integrity. In this way, live cells have a typical green nucleus (accumulate AO stain), whereas early and late apoptotic cells with condensed and fragmented chromatin incorporate EtBr stain [45]. The present data on 3-NP exposure showed apoptotic characteristics such as increased nuclear condensation, fragmentation and blebbing upon staining with Hoechst 33342 and AO/EtBr stains. However, TQ-SLNs effectively protected the cells from 3-NP mediated apoptotic events in SH-SY5Y cells via suppressing oxidative stress and mitochondrial inhibition, thus proving anti-apoptotic effect of TQ-SLNs.

Ample number of studies showed that neuronal cell cycle re-entry is associated with apoptosis in HD models [46,47]. Nevertheless, the cell cycle arrest could inhibit the cell growth and reduced the cell number in varying neurological disorders [48]. In the present study, 3-NP exposure relatively increased the accumulation of cells at G0/G1 phase and reduced the number of cell population in S and G1/M phase. Our data signifies that 3-NP may cause DNA or protein damage, chromatin destruction and manipulation of a quiescent G0 terminally differentiated neuron back into the cell cycle, thus inhibiting the entry of cells into S and G1/M phase. However, TQ-SLNs treatment govern the process of cell division in different phases of cell cycle by repairing the breakage or damages of DNA strands, causing activation of G0/G1 components of cell cycle machinery, leading to the progression of cell cycle resulting in proliferative effect.

5. CONCLUSION

Considering the above findings, it is clear that nanoformulated TQ could effectively mitigate the mitochondrial dysfunction mediated apoptosis in 3-NP challenged condition via its antioxidant and cytoprotective properties than TQ suspension in SH-SY5Y neuroblastoma cells, suggesting that this formulation may provide a beneficial role against Huntington's disease pathogenesis.

CONFLICTS OF INTEREST

The authors declare that no conflicts of interest exist.

ACKNOWLEDGEMENT

The first author is grateful to UGC-BSR for the financial support in the form of UGC-JRF Fellowship (Co/Tara/UGC-BSR/Med-Biochem/2015/613 dated 27th October 2015).

REFERENCES

[1] Brouillet E., Jacquard C., Bizat N., Blum D., 3-Nitropropionic acid: a mitochondrial toxin to uncover physiopathological mechanisms underlying striatal degeneration in Huntington's disease. J Neurochem, 95: 1521–1540, (2005)

[2] HDCRG., A novel gene containing a trinucleotide repeat that is expanded and unstable on Huntington's disease chromosomes. Cell, 72: 971–983, (1993)

[3] Moon B.B., Dahikar G.D., Ganjiwale R.O., A Review on Huntington's disease. Res J Pharm Technol, 13 (10): 4990-4995, (2020)

[4] Túnez I., Tasset I., Pérez-De La Cruz V., Santamaría A., 3-Nitropropionic acid as a tool to study the mechanisms involved in Huntington's disease: past, present and future. Molecules, 15: 878–916, (2010)

[5] Gupta S., Sharma B., Neuroprotective potential of Cilostazol in 3-NP provoked Huntington's disease-associated symptoms. Res J Pharm Technol, 14(5): 2472-2478, (2021)

[6] Kumar P., Kumar A., Effect of lycopene and epigallocatechin-3-gallate against 3-nitropropionic acid induced cognitive dysfunction and glutathione depletion in rat: a novel nitric oxide mechanism. Food Chem Toxicol, 47: 2522–2530, (2009)

[7] Khan A., Vaibhav K., Javed H., Khan M.M., Tabassum R., Ahmed M.E., et al., Attenuation of Aβ-induced neurotoxicity by thymoquinone via inhibition of mitochondrial dysfunction and oxidative stress. Mol Cell Biochem, 369: 55–65, (2012)

[8] Woo C.C., Kumar A.P., Sethi G., Tan K.H., Thymoquinone: potential cure for inflammatory disorders and cancer. Biochem Pharmacol, 83: 443–451, (2012)

[9] El-Kadi A., Kandil O., The black seed (*Nigella sativa*) and immunity: its effect on human T cell subset. Fed Proc, 46: 1222–1226, (1987)

[10] Mansour M.A., Ginawi O.T., El-Hadiyah T., El-Khatib A.S., Al-Shabanah O.A., Al-Sawaf H.A., Effects of volatile oil constituents of *Nigella sativa* on carbon tetrachloride-induced hepatotoxicity in mice: evidence for antioxidant effects of thymoquinone. Res Commun Mol Pathol Pharmacol, 110: 239–251, (2001)

[11] Ullah I., Ullah N., Naseer M.I., Lee H.Y., Kim M.O., Neuroprotection with metformin and thymoquinone against ethanol-induced apoptotic neurodegeneration in prenatal rat cortical neurons. BMC Neurosci, 13: 11, (2012)

[12] Mousavi S.H., Tayarani-Najaran Z., Asghari M., Sadeghnia H.R., Protective effect of *Nigella sativa* extract and thymoquinone on serum/glucose deprivation-induced PC12 cells death. Cell Mol Neurobiol, 30: 591–598, (2010)

[13] Alhebshi A.H., Gotoh M., Suzuki I., Thymoquinone protects cultured rat primary neurons against amyloid β-induced neurotoxicity. Biochem Biophys Res Commun, 433: 362–367, (2013)
[14] Radad K., Moldzio R., Taha M., Rausch W.D., Thymoquinone protects dopaminergic neurons against MPP+ and rotenone. Phytother Res, 23: 696–700, (2009)
[15] Hosseinzadeh H., Parvardeh S., Anticonvulsant effects of thymoquinone, the major constituent of *Nigella sativa* seeds in mice. Phytomedicine, 11: 56–64, (2004)
[16] Gilhotra N., Dhingra D., Thymoquinone produced antianxiety-like effects in mice through modulation of GABA and NO levels. Pharmacol Rep, 63: 660–669, (2011)
[17] Hosseini M., Zakeri S., Khoshdast S., Yousefian F.T., Rastegar M., Vafaee F., et al., The effects of *Nigella sativa* hydro-alcoholic extract and thymoquinone on lipopolysaccharide – induced depression like behavior in rats. J Pharm Bioallied Sci, 4: 219–225, (2012)
[18] Patil Amol M., Todkar Rohit R., Gumte Dipak S., Mohite S.K., Magdum C.S., A Review on Solid Lipid Nanoparticle. Research Journal of Pharmaceutical Dosage Forms & Technology, 8(3): 218-220, (2016)
[19] de Boer A.G., Gaillard P.J., Drug targeting to the brain. Annu Rev Pharmacol Toxicol, 47: 323–355, (2007)
[20] Surekha R., Aishwarya V., Sumathi T., Thymoquinone-loaded solid lipid nanoparticle: Formulation, characterization and *in-vitro* cell viability assay. Int J Pharm Bio Sci, 6: 449–464, (2014)
[21] Surekha R., Sumathi T., An efficient encapsulation of Thymoquinone using solid lipid nanoparticle for brain targeted drug delivery: Physicochemical characterization, pharmacokinetics and bio-distribution studies. Int J Pharm Clin Res, 8: 1616–1624, (2016)
[22] Ramachandran S., Thangarajan S., A novel therapeutic application of solid lipid nanoparticles encapsulated thymoquinone (TQ-SLNs) on 3-nitroproponic acid induced Huntington's disease-like symptoms in wistar rats. Chem-Biol Interact, 256: 25–36, (2016)
[23] Frautschy S.A., Cole G.M., Bioavailable curcuminoid formulations for treating Alzheimer's disease and other age-related disorders. United states US:2009/0324703 A1, (2009)
[24] Mustafa Rizvi S.H., Parveen A., Verma A.K., Ahmad I., Arshad M., Mahdi A.A., Aluminium induced endoplasmic reticulum stress mediated cell death in SH-SY5Y neuroblastoma cell line is independent of p53. PLoS ONE, 9: e98409, (2014)
[25] Mosmann T., Rapid colorimetric assay for cellular growth and survival: application to proliferation and cytotoxicity assays. J Immunol Methods, 65: 55–63, (1983)
[26] Mokrasch L.C., Teschke E.J., Glutathione content cultured cells and rodent brain regions: Specific fluorimetric assay. Anal Biochem, 140: 506–509, (1984)
[27] Baracca A., Sgarbi G., Solaini G., Lenaz G., Rhodamine 123 as a probe of mitochondrial membrane potential: evaluation of proton flux through F(0) during ATP synthesis. Biochim Biophys Acta, 1606: 137–146, (2003)
[28] Lowry O.H., Rosebrough N.J., Farr A.L., Randall R., Protein measurement with the Folin's phenol reagent. J Biol Chem, 193: 265–275, (1951)
[29] Polster B.M., Robertson C.L., Bucci C.J., Suzuki M., Fiskum G., Postnatal brain development and neural cell differentiation modulate mitochondrial Bax and BH3 peptide-induced cytochrome c release. Cell Death Differ, 10(3): 365–370, (2003)
[30] Zhao J., Bai Y., Zhang C., Zhang X., Zhang Y.X., Chen J., et al., Cinepazide maleate protects PC12 cells against oxygen-glucose deprivation-induced injury. Neurol Sci, 35: 875–881, (2014)
[31] Dhanalakshmi C., Manivasagam T., Nataraj J., Thenmozhi A.J., Essa M., Neurosupportive role of vanillin, a natural phenolic compound, on rotenone induced neurotoxicity in SH-SY5Y neuroblastoma cells. Evid Based Complementary Altern Med, 626028, (2015)
[32] Telford W.G., King L.E., Fraker P.J., Evaluation of glucocorticoid-induced DNA fragmentation in mouse thymocytes by flow cytometry. Cell Prolif, 24: 447–459, (1991)
[33] Federico A., Cardaioli E., Da Pozzo P., Formichi P., Gallus G.N., Radi E., Mitochondria, oxidative stress and neurodegeneration. J Neurol Sci, 322: 254–262, (2012)
[34] Lin M.T., Beal M.F., Mitochondrial dysfunction and oxidative stress in neurodegenerative diseases. Nature, 443: 787–795, (2006)
[35] Quintanilla R.A., Johnson G.V., Role of mitochondrial dysfunction in the pathogenesis of Huntington's disease. Brain Res Bull, 80: 242–247, (2009)
[36] Hariharan A., Shetty S., Shirole T., Jagtap A.G., Potential of protease inhibitor in 3-nitropropionic acid induced Huntington's disease like symptoms: mitochondrial dysfunction and neurodegeneration. Neurotoxicol, 45: 139–148, (2014)
[37] Korzeniewski C., Callewaert D.M., An enzyme-release assay for natural cytotoxicity. J Immunol Methods, 64(3): 313–320, (1983)
[38] Koh J.Y., Choi D.W., Quantitative determination of glutamate-mediated cortical neuronal injury in cell culture by lactate dehydrogenase efflux assay. J Neurosci Methods, 20: 83-90, (1987)
[39] Colle D., Santos D.B., Hartwig J.M., Godoi M., Engel D.F., de Bem A.F., et al., Succinobucol, a lipid-lowering drug, protects against 3-Nitropropionic acid-induced mitochondrial dysfunction and oxidative stress in SH-SY5Y cells via upregulation of glutathione levels and glutamate cysteine ligase activity. Mol Neurobiol, 53: 1280–1295, (2016)
[40] Condello S., Currò M., Ferlazzo N., Caccamo D., Satriano J., Lentile R., Agmatine effects on mitochondrial membrane potential and NF-κB activation protect against rotenone-induced cell damage in human neuronal-like SH-SY5Y cells. J Neurochem, 116: 67–75, (2011)
[41] Bunting J.R., Influx and efflux kinetics of cationic dye binding to respiring mitochondria. Biophys Chem, 42: 163–175, (1992)
[42] Wang C., Youle RJ., The role of mitochondria in apoptosis. Annu Rev Genet, 43: 95–118, (2009)

[43] Cummings B.S., Schnellmann R.G., Measurement of cell death in mammalian cells. Curr Protoc Pharmacol, 12: 10.1002/0471141755.ph1208s25, (2004)
[44] Schmid I., Uittenbogaart C., Jamieson B.D., Live-cell assay for detection of apoptosis by dual-laser flow cytometry using Hoechst 33342 and 7-amino-actinomycin D. Nat Protoc, 2: 187–190, (2007)
[45] Renvoizé C., Biola A., Pallardy M., Bréard J., Apoptosis: identification of dying cells. Cell Biol Toxicol, 14: 111–120, (1998)
[46] Liu K.Y., Shyu Y.C., Barbaro B.A., Lin Y.T., Chern Y., Thompson L.M., et al., Disruption of the nuclear membrane by perinuclear inclusions of mutant huntingtin causes cell-cycle reentry and striatal cell death in mouse and cell models of Huntington's disease. Hum Mol Genet, 24: 1602–1616, (2015)
[47] Fernandez-Fernandez M.R., Ferrer I., Lucas J.J., Impaired ATF6alpha processing, decreased Rheb and neuronal cell cycle re-entry in Huntington's disease. Neurobiol Dis, 41: 23–32, (2011)
[48] Tang L., Gao Y., Yan F., Tang J., Evaluation of cyclin-dependent kinase-like 1 expression in breast cancer tissues and its regulation in cancer cell growth. Cancer Biother Radiopharm, 27: 392–398, (2012)